

# Light Colored Scalar as Messenger of Up-Quark Flavor Dynamics in Grand Unified Theories

Ilja Doršner,<sup>1,\*</sup> Svjetlana Fajfer,<sup>2,3,†</sup> Jernej F. Kamenik,<sup>3,‡</sup> and Nejc Košnik<sup>3,§</sup>

<sup>1</sup>*Department of Physics, University of Sarajevo, Zmaja od Bosne 33-35, 71000 Sarajevo, Bosnia and Herzegovina*

<sup>2</sup>*Department of Physics, University of Ljubljana, Jadranska 19, 1000 Ljubljana, Slovenia*

<sup>3</sup>*J. Stefan Institute, Jamova 39, P. O. Box 3000, 1001 Ljubljana, Slovenia*

(Dated: October 31, 2018)

The measured forward-backward asymmetry in the  $t\bar{t}$  production at the Tevatron might be explained by the additional exchange of a colored weak singlet scalar. Such state appears in some of the grand unified theories and its interactions with the up-quarks are purely antisymmetric in flavor space. We systematically investigate the resulting impact on charm and top quark physics. The constraints on the relevant Yukawa couplings come from the experimentally measured observables related to  $D^0-\bar{D}^0$  oscillations, as well as di-jet and single top production measurements at the Tevatron. After fully constraining the relevant Yukawa couplings, we predict possible signatures of this model in rare top quark decays. In a class of grand unified models we demonstrate how the obtained information enables to constrain the Yukawa couplings of the up-quarks at very high energy scale.

PACS numbers: 14.65.Ha, 12.10.-g, 14.40.Lb

## I. INTRODUCTION

During the last decade, rare processes of down-type quarks have been proven instrumental in the study of physics beyond the Standard Model (SM). On the other hand, the discovery of novel effects in the up-quark sector is still often dismissed as very unlikely. In the SM in particular, rare charm processes are mostly dominated by long distance dynamics, the short distance contributions being subject to severe Glashow-Iliopoulos-Maiani cancellations. This is the case in  $D^0-\bar{D}^0$  oscillations as well as in the  $c \rightarrow u\gamma$  and  $c \rightarrow ul^+l^-$  decays. Nonetheless, the experimental situation in the charm sector is already very restrictive and present measurements constrain many models of new physics [1–7].

The heaviest up-type quark, i.e., the top quark, has been carefully investigated since its discovery in 1995. Although enormous progress has been achieved, the prospects for observing flavor changing neutral current mediated top quark decays at the Large Hadron Collider (LHC) or Tevatron are rather weak. The LHC experiments might be sensitive to the branching fractions of the order of  $10^{-5}$  or less. However, the majority of well studied models of new physics (NP) predict much weaker signals. It thus seems that the search for NP in the top sector should be directed towards other processes [8, 9].

The recent CDF measurement of a large positive forward-backward asymmetry (FBA) in the  $t\bar{t}$  production disagrees with the SM prediction and thus indicates a possible presence of NP. Among the many proposed NP scenarios aiming to explain this discrepancy, we have recently suggested [10] a theoretically well-motivated  $SU(5)$  grand unified theory (GUT) [11] model [12]. The model has an appealing feature of correlating the presence of light colored scalars stemming from a 45-dimensional Higgs representation with bounds on the proton lifetime. Namely, the aforementioned representation contains among other states two colored scalars— $\Delta_6 = (\bar{3}, 1, 4/3)$  and  $\Delta_1 = (8, 2, 1/2)$ —that have masses below or of the order of 1 TeV when partial proton decay lifetimes are predicted to be at, or slightly above, the current experimental bounds. In this regime  $\Delta_6$  can help to reconcile the SM theoretical prediction of the forward-backward asymmetry in  $t\bar{t}$  production [10, 13, 14], which is more than  $2\sigma$  below the measured value, while preserving the agreement in the total  $t\bar{t}$  production cross section. On the other hand, the contributions from  $\Delta_1$  are required to be suppressed [10].

Relatively light colored scalars may also arise in other extensions of the SM. Generically, lower bounds of their masses can be inferred from their strong interaction mediated production at hadron colliders. In addition however, their couplings to SM matter fields will induce contributions to flavor observables. We investigate constraints and predictions of flavor observables in the up-quark sector in the presence of a color triplet weak singlet scalar with hypercharge  $4/3$ . Furthermore, we address the resulting constraints on the Yukawa sector of a particular class of

\* Electronic address: ilja.dorsner@ijs.si

† Electronic address: svjetlana.fajfer@ijs.si

‡ Electronic address: jernej.kamenik@ijs.si

§ Electronic address: nejc.kosnik@ijs.si

GUT models that employ the 45-dimensional  $SU(5)$  Higgs representation containing such state [15]. As has been noticed recently,  $\Delta_6$  exchange does not contribute to  $d = 6$  proton decay operators [16] and can thus be light.

In Section II, we describe our framework. The  $D^0 - \bar{D}^0$  constraints are studied in Section III. Constraints coming from the Tevatron single top and di-jet production cross-section measurements are presented in Section IV. Resulting predictions for rare top decays are given in Section V, while implications of phenomenologically deduced constraints for the entire up-quark Yukawa sector in GUT models are addressed in Section VI. Discussion and summary are presented in Section VII.

## II. FRAMEWORK

The color triplet scalar we study appears in theoretically well-motivated class of  $SU(5)$  models. Namely, it is a part of a 45-dimensional Higgs representation, which has been frequently used in GUT model building to accommodate known fermion masses, improve unification of gauge couplings, and address proton decay constraints [12, 15, 17–20]. Recall that matter of the SM is assigned to a 10- and 5-dimensional  $SU(5)$  representations, i.e.  $\mathbf{10}_i = (1, 1, 1) \oplus (\bar{3}, 1, -2/3) \oplus (3, 2, 1/6)$  and  $\bar{\mathbf{5}}_i = (1, 2, -1/2) \oplus (\bar{3}, 1, 1/3)$  where  $i = 1, 2, 3$  denotes generation index. It couples to the 45-dimensional Higgs representation  $\mathbf{45}$  through the following operators

$$V_{45}^{\text{matter}} = (Y_1)^{ij} (\mathbf{10}^{\alpha\beta})_i (\bar{\mathbf{5}}_\delta)_j \mathbf{45}_{\alpha\beta}^{*\delta} + (Y_2)^{ij} \epsilon_{\alpha\beta\gamma\delta\epsilon} (\mathbf{10}^{\alpha\beta})_i (\mathbf{10}^{\zeta\gamma})_j \mathbf{45}_{\zeta}^{\delta\epsilon}. \quad (1)$$

Lepton and baryon number violating Yukawa couplings of  $\Delta_6$  in the interaction basis are

$$\mathcal{L}_{\Delta_6} = \sqrt{2} [(Y_2)_{ij} - (Y_2)_{ji}] \epsilon_{abc} \bar{u}_{ia} P_L u_{jb}^c \Delta_6^c + (Y_1)^{ij} \bar{e}_i P_L d_{ja}^c \Delta_6^{a*} + \text{H.c.}, \quad (2)$$

where  $a, b, c$  are color indices, while  $i, j$  denote flavors. Note that the antisymmetric nature of the  $\Delta_6$  coupling to the up-quark sector in flavor space is dictated by group theory. Yukawa couplings of  $\Delta_6$  to diquarks in the physical basis, i.e., the up-quark mass eigenstate basis, acquire a unitary rotation ( $U_R$ ), which however does not spoil the antisymmetry in flavor indices. Hence, we define

$$g_6^{ij} \equiv 2\sqrt{2} \left[ U_R^\dagger (Y_2 - Y_2^T) U_R^* \right]^{ij}, \quad g_6^{ij} = -g_6^{ji}, \quad (3)$$

altogether with three independent parameters:  $g_6^{12}$ ,  $g_6^{23}$ , and  $g_6^{13}$ . It is the antisymmetry of  $g_6$  that is responsible for the absence of the  $d = 6$  operators due to  $\Delta_6$  exchange that would otherwise contribute to proton decay [16]. In what follows we focus our attention on phenomenological constraints of these entries.

Note that a tree-level exchange of  $\Delta_6$  contributes to  $t\bar{t}$  production cross-section in the  $u$ -channel. It was emphasized in [10] that  $\Delta_6$  at and below 1 TeV can enhance the SM prediction of the forward-backward asymmetry  $A_{FB}^{t\bar{t}}$  while not altering the production cross-section  $\sigma_{t\bar{t}}$ . This has been achieved by finding the parameter space of  $m_{\Delta_6}$  and coupling  $g_6^{13}$ , contributing to partonic subprocess  $u\bar{u} \rightarrow t\bar{t}$ , in  $p\bar{p}$  collisions, which together with SM reproduce the measured values of  $A_{FB}^{t\bar{t}}$  and  $\sigma_{t\bar{t}}$ . The region where experimental constraints can be satisfied within  $1\sigma$  roughly corresponds to a region, where mass of  $\Delta_6$  and the coupling  $g_6^{13}$  are correlated as

$$|g_6^{13}| = 0.9(2) + 2.5(4) \frac{m_{\Delta_6}}{1 \text{ TeV}}. \quad (4)$$

We investigate the bounds on the remaining two couplings ( $g_6^{12}$ ,  $g_6^{23}$ ) in the following sections.

## III. $D^0 - \bar{D}^0$ MIXING CONSTRAINTS

Mixing of neutral charm mesons is sensitive to interactions which change charm flavor by 2 units. Scalar  $\Delta_6$ , if light enough, may strongly contribute to effective  $|\Delta C| = 2$  interactions and expose its Yukawa couplings to the up-type quarks in  $D^0 - \bar{D}^0$  mixing. In this section we study the contribution of  $\Delta_6$  to  $D^0 - \bar{D}^0$  mixing observables and place constraints on its Yukawa coupling to  $c$  and  $t$  quarks— $g_6^{23}$ .

The  $D^0 - \bar{D}^0$  mixing matrix element of  $|\Delta C| = 2$  Hamiltonian is split into dispersive ( $M_{12}$ ) and absorptive ( $\Gamma_{12}$ ) parts as following

$$\langle D^0 | \mathcal{H} | \bar{D}^0 \rangle = M_{12} - \frac{i}{2} \Gamma_{12}, \quad (5)$$

and due to the (anti)hermiticity of  $M_{ij}$  ( $i/2\Gamma_{ij}$ ) also  $\langle \bar{D}^0 | \mathcal{H} | D^0 \rangle = M_{12}^* - \frac{i}{2}\Gamma_{12}^*$  holds. Two dimensionless parameters describe magnitudes of the dispersive ( $x_{12}$ ) and the absorptive ( $y_{12}$ ) part while a relative phase between  $M_{12}$  and  $\Gamma_{12}$  would signal  $CP$  violation [3]

$$x_{12} = \frac{2|M_{12}|}{\Gamma}, \quad y_{12} = \frac{|\Gamma_{12}|}{\Gamma}, \quad \phi_{12} = \arg(M_{12}/\Gamma_{12}). \quad (6)$$

Here  $\Gamma$  is the average decay width of neutral  $D$  mesons. Contributions to the absorptive part  $y_{12}$  come from on-shell intermediate states and are thus accounted for by SM. On the other hand, in the presence of  $\Delta_6$   $x_{12}$  and  $\phi_{12}$  are affected by the box diagrams consisting of  $\Delta_6$  and  $t$ -quark exchanges which mediate  $D^0-\bar{D}^0$  transitions, as shown on Fig. 1. Since the preferred mass of  $\Delta_6$  is between 300 GeV and 1 TeV in order to explain the  $t\bar{t}$  asymmetry [10], we

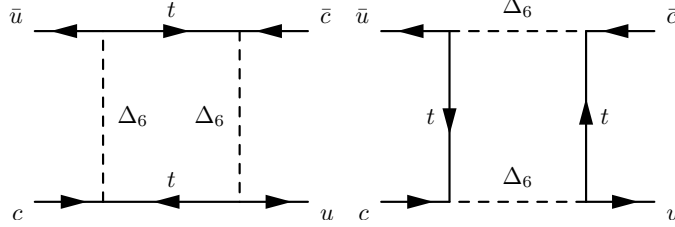


Figure 1. Contribution of order  $(g_6^{13}g_6^{23*})^2$  to  $\Delta C = 2$  effective Hamiltonian.

can safely integrate out both the top quark and  $\Delta_6$  at a common scale  $\mu = m_{\Delta_6}$ . Leading order matching onto the effective theory generates a single operator, denoted in the literature as  $Q_6$  [21]

$$\mathcal{H}(\mu = m_{\Delta_6}) = C_6(m_{\Delta_6})Q_6, \quad Q_6 = (\bar{u}_R\gamma^\mu c_R)(\bar{u}_R\gamma_\mu c_R), \quad (7)$$

with the corresponding Wilson coefficient

$$C_6(m_{\Delta_6}) = \frac{(g_6^{13}g_6^{23*})^2 h(m_{\Delta_6}^2/m_t^2)}{32\pi^2 m_t^2}, \quad h(x) = \frac{x^2 - 2x \log x - 1}{(x-1)^3}. \quad (8)$$

Effective Hamiltonian is evolved down to the charm scale  $\mu_D = 2$  GeV using the leading-log anomalous dimension. The multiplicative renormalization factor of  $C_6$  in our case is adopted from Ref. [1] and reads

$$r(\mu_D, m_{\Delta_6}) = \left( \frac{\alpha_S^{(5)}(m_{\Delta_6})}{\alpha_S^{(5)}(m_b)} \right)^{6/23} \left( \frac{\alpha_S^{(4)}(m_b)}{\alpha_S^{(4)}(\mu_D)} \right)^{6/25}. \quad (9)$$

The nonperturbative bag parameter  $B_D$  corrects the vacuum insertion approximation value of the mixing matrix element

$$\langle D^0 | (\bar{u}_R\gamma^\mu c_R)(\bar{u}_R\gamma_\mu c_R) | \bar{D}^0 \rangle = \frac{2}{3} m_D^2 f_D^2 B_D. \quad (10)$$

We use the value  $B_D(\mu_D = 2 \text{ GeV}) = 0.785$  calculated on the lattice employing quenched Wilson fermions [22]. For the decay constant we use the CLEO measured value  $f_D = 0.206 \text{ GeV}$  [23].

Experimentally,  $D^0-\bar{D}^0$  mixing has now been confirmed, while  $CP$  violation is still consistent with zero, as is evident from the latest HFAG [24] average which assumes no direct  $CP$  violation

$$x = (0.59 \pm 0.20)\%, \quad y = (0.81 \pm 0.13)\%, \quad (11a)$$

$$|q/p| = 0.98_{-0.14}^{+0.15}, \quad \phi = -0.051_{-0.115}^{+0.112}. \quad (11b)$$

The assumption of negligible direct  $CP$  violation resides on the fact that  $\Delta_6$  cannot contribute to  $\Gamma_{12}$ , and that in the SM  $CP$  violation is very small [3]. In this case, the four measured parameters are governed by the three independent theoretical quantities (6), implying redundancy of one of the four experimental parameters. Indeed the values of  $|q/p|$  and  $\phi$  are found to be strongly correlated in the HFAG fit (11) with correlation coefficient of 0.614 [24]. We choose to extract  $x_{12}$  and  $\phi_{12}$  from  $x$ ,  $y$ , and  $|q/p|$  using the following relations [3, 25]

$$x_{12}^2 = \frac{(|q/p|^2 + 1)^2 x^2 + (1 - |q/p|^2)^2 y^2}{4|q/p|^2}, \quad (12)$$

$$\sin^2 \phi_{12} = \frac{(1 - |q/p|^4)^2 (x^2 + y^2)^2}{16|q/p|^4 x^2 y^2 + (1 - |q/p|^4)^2 (x^2 + y^2)^2}. \quad (13)$$

Imaginary part of  $M_{12}$  is directly accessible in the product

$$x_{12} \sin \phi_{12} = \frac{2 \operatorname{Im} M_{12}}{\Gamma}, \quad (14)$$

which we constrain, along with  $x_{12}$ , from the HFAG values (11). The 1 and  $2\sigma$  confidence levels of  $x_{12}$  and  $x_{12}|\sin \phi_{12}|$  are shown on Fig. 2, whereas the upper bounds at 95 % ( $2\sigma$ ) confidence level are

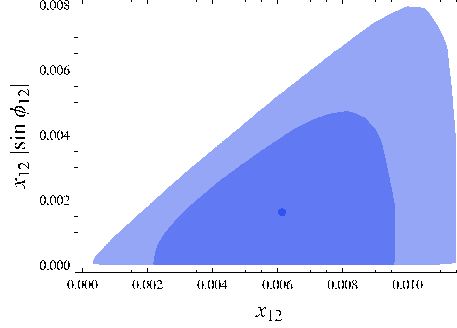


Figure 2. The 1 and  $2\sigma$  confidence level regions (dark and light-shaded regions, respectively) in the plane  $x_{12}$ - $x_{12}|\sin \phi_{12}|$ .

$$x_{12} < 9.6 \times 10^{-3}, \quad x_{12}|\sin \phi_{12}| < 4.4 \times 10^{-3}. \quad (15)$$

The imaginary part of  $M_{12}$  originates from relative phase between the  $g_6^{23}$  and  $g_6^{13}$ , namely,

$$\operatorname{Im} [(g_6^{13} g_6^{23*})^2] = |g_6^{13}|^2 |g_6^{23}|^2 \sin(2\omega), \quad (16)$$

where  $\omega$  is the difference between phases of  $g_6^{13}$  and  $g_6^{23}$ . Using the central value for  $|g_6^{13}|$ , as given in Eq. (4), we find the region of  $|g_6^{23}|$ , which is limited from above by the 95 % upper bounds (15), and is shown in Fig. 3. The bound

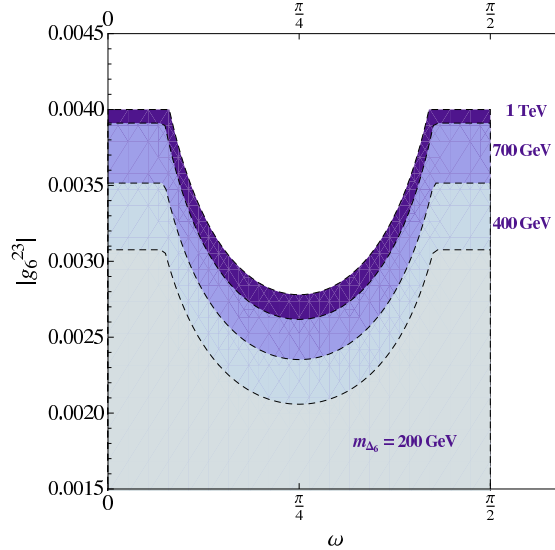


Figure 3. Allowed regions of  $|g_6^{23}|$  and  $\omega$  for different values of  $m_{\Delta_6}$ .

on  $x_{12}|\sin \phi_{12}|$  is stronger, except in the regions close to  $\omega = 0$  or  $\pi/2$ , where bound on  $x_{12}$  dominates. Apparent nondecoupling, i.e., strong bound even for large masses  $m_{\Delta_6}$ , is due to linear dependence of  $|g_6^{13}|$  on  $m_{\Delta_6}$  (see Eq. (4)). We obtain a robust  $2\sigma$  bound in the region of interest  $m_{\Delta_6} < 1$  TeV:

$$|g_6^{23}| < 0.0038, \quad (17)$$

regardless of complex phases, thus allowing also for finely tuned phase  $\omega$ .

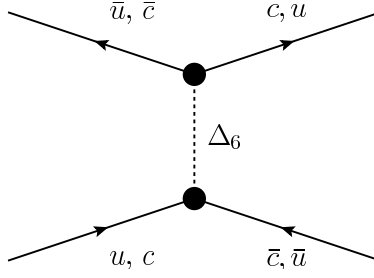


Figure 4. Partonic contribution to di-jet production at the Tevatron from a  $u$ -channel  $\Delta_6$  exchange. The analogous  $s$ - and  $t$ -channel contributions can simply be obtained via crossing.

One can extract the product  $|g_6^{13}g_6^{23*}|$  also from the radiative  $c \rightarrow u\gamma$  decay, where the  $\Delta_6$ -induced effective Hamiltonian reads

$$\mathcal{H}^{c \rightarrow u\gamma} = \frac{g_6^{13}g_6^{23*}f(m_{\Delta_6}^2/m_t^2)}{6m_t^2} \times \frac{em_c}{(4\pi)^2} (\bar{u}_R \sigma^{\mu\nu} c_L) F_{\mu\nu}, \quad (18)$$

with  $F_{\mu\nu}$ ,  $e$  the electromagnetic tensor and coupling, whereas function  $f$  is

$$f(x) = \frac{2x^3 + 3x^2 - 6x^2 \log x - 6x + 1}{(x-1)^4}. \quad (19)$$

However, using bounds on the couplings (Eqns. (17) and (4)) we find

$$\Gamma^{c \rightarrow u\gamma} / \Gamma_{D^0} \lesssim 10^{-10}, \quad (20)$$

whereas the SM resonant contributions to  $D \rightarrow V\gamma$  and  $D \rightarrow P\ell^+\ell^-$  ( $P$  and  $V$  denote pseudoscalar and vector mesons) are of the order of  $10^{-6}$  [26–28]. This implies that radiative decays offer a far weaker constraint than the measured  $D^0$ – $\bar{D}^0$  observables.

#### IV. BOUNDS ON $g_6^{12}$

In this section we consider bounds on the coupling  $g_6^{12}$  coming from the CDF search for resonances in the invariant mass spectrum of di-jets [29] as well as from the single top production cross-section measurements at the Tevatron [30]. The first measurement constrains the  $|g_6^{12}|$  coupling directly since the process can be mediated by  $\Delta_6$  through  $s$ -,  $u$ - and  $t$ -channel exchange diagrams (see Fig. 4) interfering with leading order (LO) QCD contributions at the partonic level. The resulting partonic  $u\bar{u} \rightarrow c\bar{c}$  differential cross-section from the  $u$ -channel  $\Delta_6$  contribution interfering with the  $s$ -channel single gluon exchange is

$$\begin{aligned} \frac{d\sigma_6^{u\bar{u} \rightarrow c\bar{c}}(\hat{s})}{d\hat{t}} &= \frac{d\sigma_{SM}^{u\bar{u} \rightarrow c\bar{c}}(\hat{s})}{d\hat{t}} + \frac{|g_6^{12}|^4}{48\pi\hat{s}^2} \frac{\hat{u}^2}{(m_{\Delta_6}^2 - \hat{u})^2 + \Gamma_{\Delta_6}^2} \\ &\quad - \frac{\alpha_s |g_6^{12}|^2}{9\hat{s}^3} \frac{\hat{u}^2 (m_{\Delta_6}^2 - \hat{u})}{(m_{\Delta_6}^2 - \hat{u})^2 + \Gamma_{\Delta_6}^2}, \end{aligned} \quad (21)$$

where  $\hat{s} = (p_{\bar{u}} + p_u)^2$ ,  $\hat{t} = (p_u - p_c)^2$ ,  $\hat{u} = (p_{\bar{u}} - p_c)^2$ . The expression for the  $c\bar{c} \rightarrow u\bar{u}$  is identical, while contributions from the related  $u\bar{c} \rightarrow u\bar{c}$ ,  $c\bar{u} \rightarrow c\bar{u}$ ,  $uc \rightarrow uc$  and  $\bar{u}\bar{c} \rightarrow \bar{u}\bar{c}$  processes can be obtained via crossing. Since the last two contributions involve  $\Delta_6$  exchange in the  $s$ -channel, we have included the  $\Delta_6$  total width  $\Gamma_{\Delta_6}$  as the regulator of the on-shell pole in all expressions. We assume that  $\Gamma_{\Delta_6}$  is dominated by the three decay channels to pairs of quarks  $ut$ ,  $ct$  and  $uc$ . For the  $\Delta_6 \rightarrow tq_i$  ( $q_1, q_2 = u, c$ ) channels we keep the top quark mass dependence in the partial width

$$\Gamma(\Delta_6 \rightarrow tq_i) = \frac{|g_6^{i3}|^2 (m_{\Delta_6}^2 - m_t^2)^2}{16\pi m_{\Delta_6}^3}, \quad (22)$$

while we neglect quark masses in the analogous expression for the  $\Delta_6 \rightarrow uc$  channel. As shown in the previous section, the  $tc$  channel is severely constrained by experimental results on  $D^0$ – $\bar{D}^0$  oscillations and can be neglected. In order to

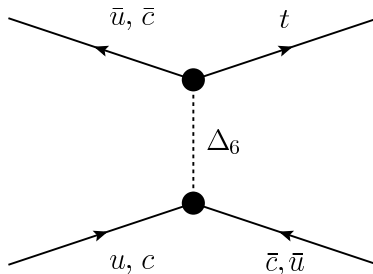


Figure 5. Partonic contribution to the single top production at the Tevatron from a  $u$ -channel  $\Delta_6$  exchange. The analogous  $s$ -channel contribution can simply be obtained by crossing.

compare with the experimental results [29] we first compute the hadronic di-jet production invariant mass spectrum by convoluting the LO QCD partonic differential cross-section including the above described tree-level  $\Delta_6$  contributions with the CTEQ5 [31] set of parton distribution functions (PDFs) at the factorization and  $\alpha_s$  renormalization scale set to  $\mu_F = \mu_R = E_T$ , where  $E_T$  is the transverse energy of the final state di-jet. (We employ  $\alpha_s(m_Z) = 0.117$  [32].) We also require both jets to have rapidity  $|y| < 1$ . Then we reweigh our results so that our SM predictions (with  $g_6^{12} = 0$ ) match the complete NLO QCD results computed with FastNLO [33], CTEQ6.1 [34] set of PDFs and appropriate jet algorithms as used in the original CDF analysis [29]. Finally, we turn on  $\Delta_6$  contributions and compare the resulting spectra with published CDF results. Assuming that  $\Delta_6$  is responsible for the measured large FBA in top quark pair production at the Tevatron [35–37], combined with the measured total  $t\bar{t}$  production cross-section as well as the top pair invariant mass spectrum, leads to the  $g_6^{13}$  coupling and  $\Delta_6$  mass satisfying the approximate relation given in Eq. (4). Then the total  $\Delta_6$  decay width in the interesting region of  $|g_6^{12}|$  is comparable with the experimental di-jet invariant mass bin size. We obtain the bounds on  $|g_6^{12}|$  as a function of  $m_{\Delta_6}$  by comparing the obtained theoretical spectrum for given values of  $\Delta_6$  parameters with the experimental measurement. The results are shown as the purple shaded area in Fig. 6.

The single top production cross-section is sensitive to the product of  $|g_6^{12}g_6^{13*}|$  (and also  $|g_6^{12}g_6^{23*}|$ , which, however, is more severely constrained by  $D^0$ – $\bar{D}^0$  oscillation measurements and we neglect it in what follows) since it proceeds at partonic level through  $s$ - and  $u$ -channel  $\Delta_6$  exchange diagrams (see Fig. 5). The resulting  $u$ -channel partonic contribution to  $u\bar{u} \rightarrow t\bar{c}$  has the form

$$\frac{d\sigma^{u\bar{u} \rightarrow t\bar{c}}}{d\hat{t}} = -\frac{|g_6^{13*}g_6^{12}|^2}{48\pi\hat{s}^2} \frac{(\hat{s} + \hat{t})\hat{u}}{(\hat{u} - m_{\Delta_6}^2)^2 + \Gamma_{\Delta_6}^2}, \quad (23)$$

where now  $\hat{s} = (p_{\bar{u}} + p_u)^2$ ,  $\hat{t} = (p_u - p_t)^2$ ,  $\hat{u} = (p_{\bar{u}} - p_t)^2$ . The analogous  $uc \rightarrow tu$  expression is related to it via crossing. A bound on  $|g_6^{12}|$  can then be obtained by using the  $t\bar{t}$  FBA preferred values of  $|g_6^{13}|$  in Eq. (4). Since all the current experimental measurements of single top production use sophisticated multivariate analysis techniques it is difficult to compare  $\Delta_6$  contributions directly with their data. Therefore we employ a conservative approach and only compare NP contributions with the experimental error on the combined Tevatron result for the total single-top production cross-section (summed over both  $t$  and  $\bar{t}$ ) of  $\sigma_{1t} = 2.76_{-0.47}^{+0.58}$  pb [30]—we require the  $\Delta_6$  mediated hadronic production cross-section, which we denote  $\Delta\sigma_{1t}$ , to be smaller than 1 pb at 95% confidence level. A recent dedicated D0 analysis of NP mediated single top production obtained even stricter limits on the anomalous single top production cross-section [38], however their results are not directly applicable to our case due to different partonic initial and final states as well as different kinematics. We compute the NP-mediated single top production by again convoluting the partonic differential cross-section with the appropriate PDFs at the factorization and  $\alpha_s$  renormalization scale set to  $\mu_F = \mu_R = E_T$  and then integrating over the available hadronic phase-space. Since in this case there are no contributions due to the SM-NP interference, the  $\Delta_6$  mediated single top production cross-section (and the associated constraint) scales quadratically with  $|g_6^{12}g_6^{13*}|$ . Using the  $t\bar{t}$  forward backward asymmetry preferred values of  $|g_6^{13}|$  in Eq. (4) we obtain the bounds on  $|g_6^{12}|$  shaded in blue in Fig. 6.

## V. PREDICTIONS FOR RARE TOP QUARK DECAYS

Having obtained the upper bounds on  $|g_6^{12}|$  and  $|g_6^{23}|$  we can now assess the prospects of observing radiative top quark decays at the LHC. We predict decay widths of processes with an up-type quark and a photon or a gluon in the final state.

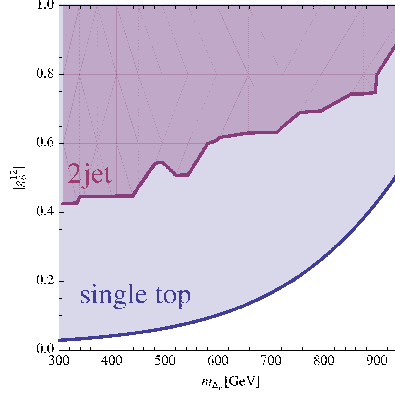


Figure 6. Constraint on the  $|g_6^{12}|$  coupling and  $\Delta_6$  mass from the single top production and di-jet at the Tevatron. The shaded areas are excluded.

The  $\Delta_6$ -induced effective Hamiltonian for a top quark decay to a light up-type quark (massless  $c$  or  $u$ ) and a single photon or a gluon reads

$$\begin{aligned} \mathcal{H}^{t \rightarrow q_i \gamma, q_i G} = & g_6^{12} \frac{F^\gamma(m_{\Delta_6}^2/m_t^2)}{3m_t^2} \frac{em_t}{(4\pi)^2} [g_6^{13*}(\bar{c}_R \sigma^{\mu\nu} t_L) - g_6^{23*}(\bar{u}_R \sigma^{\mu\nu} t_L)] F_{\mu\nu} \\ & - g_6^{12} \frac{F^G(m_{\Delta_6}^2/m_t^2)}{2m_t^2} \frac{gm_t}{(4\pi)^2} [g_6^{13*}(\bar{c}_R \sigma_{\mu\nu} T^A t_L) - g_6^{23*}(\bar{u}_R \sigma_{\mu\nu} T^A t_L)] G_A^{\mu\nu}, \end{aligned} \quad (24)$$

where  $e$ ,  $F_{\mu\nu}$  and  $g$ ,  $G_{\mu\nu}^A$  are electromagnetic and color coupling constant and field tensors, respectively. Dependence on  $m_{\Delta_6}$  is ascribed to

$$F^\gamma(x) = -2x - 3 - 2(x-1)x \log \frac{x-1}{x} + 4x \text{Li}_2(1/x), \quad (25a)$$

$$F^G(x) = 2x + 2x(x-1) \log \frac{x-1}{x} - x \text{Li}_2(1/x). \quad (25b)$$

The light quark in the final state, regardless of being either  $c$  or  $u$ , couples via  $g_6^{12}$  to the light quark and  $\Delta_6$  in the loop. The top quark, however, couples predominantly to  $u$  and  $\Delta_6$  (its coupling to  $c$  and  $\Delta_6$  is suppressed by the smallness of  $|g_6^{23}|$ ) in the loop and thus  $t \rightarrow u\gamma, uG$  decay widths are suppressed by a factor of  $|g_6^{23}/g_6^{13}|^2 \sim 10^{-6}$  with respect to  $t \rightarrow c\gamma, cG$  widths. For decays with a  $c$ -quark in the final state we find at leading order in  $\alpha_S$

$$\Gamma^{t \rightarrow c\gamma} = \frac{\alpha |g_6^{12} g_6^{13}|^2 m_t}{2304\pi^4} [F^\gamma(m_{\Delta_6}^2/m_t^2)]^2, \quad \Gamma^{t \rightarrow cG} = \frac{\alpha_S |g_6^{12} g_6^{13}|^2 m_t}{768\pi^4} [F^G(m_{\Delta_6}^2/m_t^2)]^2. \quad (26)$$

For  $\Delta_6$  masses below 1 TeV the expressions (26) lead to branching fractions' upper limit of the order of  $10^{-9}$  for both  $t \rightarrow c\gamma$  and  $t \rightarrow cG$ . Independently of the coupling constant values, the width of the photonic channel is 30–40 % larger than the  $t \rightarrow cG$  width. QCD corrections for these processes are known [39–41]. For the  $t \rightarrow cG$  channel they amount to 20 % enhancement in the branching fraction. On the other hand, the smallness of the gluonic rate leads to negligible effects in the  $t \rightarrow c\gamma$  branching fraction [40].

Interestingly, the ratio of tree-level contributions of  $\Delta_6$  in single  $t$  production cross-section  $\Delta\sigma_{1t}$  (see Eq.(23)) and  $t \rightarrow c\gamma$  or  $t \rightarrow cG$  decay width is completely independent of  $g_6$  couplings. On the other hand, the ratio  $\Gamma_{t \rightarrow cG, c\gamma}/\Delta\sigma_{1t}$  exhibits a nontrivial  $\Delta_6$  mass dependence, as shown in Fig. 7.

## VI. PREDICTION FOR THE UP-QUARK YUKAWA SECTOR

The fact that all three entries of  $g_6$  are either fixed or bounded through processes that involve the same scalar field, i.e.,  $\Delta_6$ , presents us with a unique opportunity to put constraints on relevant Yukawa coupling constants within a large class of GUT models in the up-quark sector at the very high scale as we show next.

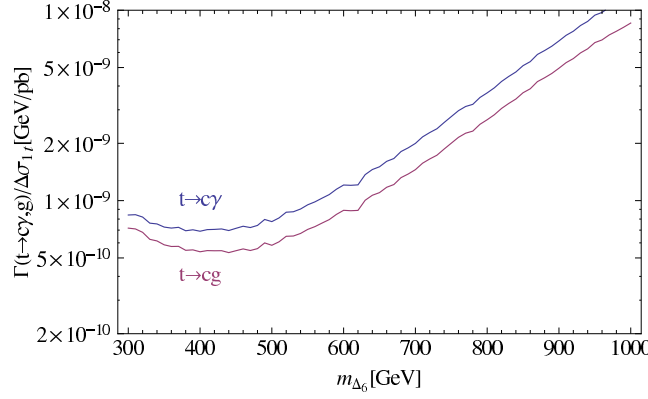


Figure 7. Ratio of top quark decay widths  $t \rightarrow c\gamma, cG$  and  $\Delta_6$  contribution to the single top production at the Tevatron. See text for explanation.

We mentioned already that  $\Delta_6$  is a part of a 45-dimensional Higgs representation of  $SU(5)$  and the 45-dimensional Higgs representation, i.e., **45**, is frequently used in  $SU(5)$  GUT models. The relevant coupling—already given in Eq. (1)—basically sets a model dependent lower bound on a vacuum expectation value of the Higgs doublet that resides in **45**.

We find that at least one component of  $g_6$  that describes the couplings of  $\Delta_6$  to the up-quarks must differ from zero to accommodate forward-backward asymmetry in top quark pair production at the Fermilab Tevatron. But,  $g_6$  is related, via Eq. (3), to the coupling of the Higgs doublet in the 45-dimensional representation to matter. This antisymmetric contribution, however, is not sufficient to generate viable up-quark mass spectrum. Namely, one 5-dimensional Higgs, i.e., **5**, is also needed to generate viable up-quark mass spectrum via renormalizable set of  $SU(5)$  Yukawa coupling contractions. The relevant contraction of **5** with matter is  $\epsilon_{\alpha\beta\gamma\delta\epsilon}(Y'_2)_{ij}(\mathbf{10}^{\alpha\beta})_i(\mathbf{10}^{\gamma\delta})_j(\mathbf{5})^\epsilon$ . The up-quark mass matrix at the GUT scale reads

$$M_U = [4(Y_2'^T + Y_2')v_5 - 8(Y_2^T - Y_2)v_{45}] / \sqrt{2}, \quad (27)$$

where  $\langle \mathbf{5} \rangle^5 = \sqrt{2}v_5$  and  $\langle \mathbf{45} \rangle_1^{51} = \langle \mathbf{45} \rangle_2^{52} = \langle \mathbf{45} \rangle_3^{53} = \sqrt{2}v_{45}$  represent appropriate vacuum expectation values. (Note,  $2|v_5|^2 + 48|v_{45}|^2 = v^2$ , where  $v = 246$  GeV.)  $Y'_2$  and  $Y_2$  are in general arbitrary  $3 \times 3$  Yukawa matrices.

We can now show that constraints on  $g_6$  immediately translate into constraints on symmetric coupling contribution in Eq. (27). Namely, if we go to the basis where the down-quarks mass matrix is diagonal we obtain the following two equations

$$4S' = U^\dagger M_U^{diag} + M_U^{diag} U^* \quad (28a)$$

$$4A' = U^\dagger M_U^{diag} - M_U^{diag} U^*, \quad (28b)$$

where  $U = \tilde{V}_{CKM} U_R$  and  $M_U^{diag}$  is a diagonal up-quark mass matrix. Note that  $\tilde{V}_{CKM} = U_1 V_{CKM} U_2$  is proportional to Cabibbo-Kobayashi-Maskawa (CKM) matrix  $V_{CKM}$  apart from five phases that are present at the GUT scale contained within diagonal unitary matrices  $U_1$  and  $U_2$ .  $A' (= 2\sqrt{2}U_R^\dagger(Y_2 - Y_2^T)U_R^* v_{45})$  and  $S' (= \sqrt{2}U_R^\dagger(Y_2'^T + Y_2')U_R^* v_5)$  are antisymmetric and symmetric contributions, respectively.  $U_R$ , again, is an arbitrary unitary matrix. These relations hold at the GUT scale whereas our constraints on  $g_6$  originate from the low-energy phenomenology. If we run  $g_6$  constraints as well as relevant fermion masses and their mixing parameters from electroweak scale to the GUT scale we would finally have  $A' = g_6 v_{45}$ . It is this relation that lets us deduce generic properties of the symmetric contribution  $S'$  and thus pinpoint the texture of the up-quark Yukawa couplings.

We now state several important generic features of the Yukawa coupling constants in the up-quark sector as implied by our constraints on  $g_6$ . Firstly, the ratio  $|S'_{13}|/|A'_{13}|$  is equal to one at all instances. This is due to the fact that one of the  $|A'|$  entries, i.e., the one proportional to  $|g_6^{13}|$  is fixed phenomenologically and is significantly larger than the upper bounds on the other two entries of  $|A'|$ . Further, both  $|A'_{13}|$  and  $|S'_{13}|$  are well approximated with the same product  $|U_{31}|m_t$  since  $M_U^{diag}$  is highly hierarchical matrix. Since  $|g_6^{13}|$  is fixed and larger than both  $|g_6^{12}|$  and  $|g_6^{23}|$ , we find  $|U_{31}|/v_{45}$  to be just a constant for a given  $m_{\Delta_6}$  while  $|S'_{13}| = |A'_{13}|$ .

Secondly, since  $|A'_{23}|$  should phenomenologically be much smaller when compared with  $|A'_{13}|$  it is clear that  $|U_{32}|$  entry must be very small in order to suppress the first term in  $A'_{23} = U_{32}^* m_t - U_{23}^* m_c$  equality. As a consequence, there is thus a correlation between  $|U_{31}|$  and  $|U_{33}|$  due to unitarity of  $U$ . This correlation also implies that the ratio  $|S'_{33}|/|A'_{13}|$



should depend only on  $|U_{31}|$  (or, interchangeably,  $v_{45}$ ). In fact, analytically we find  $|S'_{33}|/|A'_{13}| \approx 2\sqrt{1 - |U_{31}|^2}/|U_{31}|$ . We plot  $|U_{31}|$  vs.  $|S'_{33}|/|A'_{13}|$  as obtained in our numerical analysis superimposed over  $2\sqrt{1 - |U_{31}|^2}/|U_{31}|$  in Fig. 8. Squares represent satisfactory numerical solutions of Eqns. (28) that satisfy all other phenomenological constraints. We describe our numerical procedure in detail later on. The most important facts we can conclude from Fig. 8 are that  $|U_{32}|$  is indeed negligible,  $|S'_{33}|$  is determined for a given value of  $|U_{31}|$  and  $|S'_{33}|$  is usually smaller than or, at most, comparable with  $|A'_{13}|$ .

Thirdly, there is a connection between  $|S'_{12}| = |U_{21}^* m_c + U_{12}^* m_u|$  and  $|A'_{12}| = |U_{21}^* m_c - U_{12}^* m_u|$ . Namely, if  $|U_{31}|$  is small then unitarity makes  $|U_{21}|$  large which in turn implies that the ratio  $|S'_{12}|/|A'_{12}|$  tends to one. In the other extreme, when  $|U_{31}|$  approaches one,  $|U_{21}|$  goes to zero and there is a possible interference between the two terms in  $|S'_{12}|$  and  $|A'_{12}|$  which makes their ratio deviate from one but not by a large amount. This behavior is depicted in Fig. 9 where we plot  $\log |S'_{12}|/|A'_{12}|$  vs.  $|U_{31}|$ . Clearly,  $|S'_{12}|$  and  $|A'_{12}|$  are within a factor of three from each other for all values of  $|U_{31}|$ . Note,  $|U_{31}|$  cannot be arbitrarily small as is also evident in Figs. 8 and 9. In fact, when  $|U_{31}| \rightarrow 0$ , with  $|U_{32}|$  negligible,  $|A'_{13}| \rightarrow 0$ .

Fourthly, there exist a correlation that concerns  $|S'_{11}|$  and  $|S'_{22}|$ . What we find is that, due to the fact that  $|U_{32}|$  is negligible, unitarity of  $U$  demands that  $|S'_{11}|/|S'_{22}| \rightarrow m_u/m_c$  for  $|U_{31}| \rightarrow 0$ . We plot this behavior in Fig. 10, where we plot  $\log |S'_{11}|/|S'_{22}|$  vs.  $|U_{31}|$ . It is clear from Fig. 10 that  $|U_{31}| \neq 1$  yields unique value for  $|S'_{11}|/|S'_{22}|$ . Recall, in that regime, the ratio  $|S'_{12}|/|A'_{12}|$  is also uniquely determined.

Finally, there exists a model dependent lower bound (and upper bound) on  $v_{45}$  from the charged lepton and down-quark sector in models with the 45-dimensional Higgs. However, due to the fact that the **45** contraction on its own cannot provide viable up-quark masses it is clear that there will also exist an upper bound on  $v_{45}$  from the observed up-quark sector masses. The novelty is that this upper bound will be  $m_{\Delta_6}$  dependent since the phenomenologically viable form of  $g_6$  is  $m_{\Delta_6}$  dependent as given in Eq. (4). We show the upper bound on  $v_{45}$  as a function of  $m_{\Delta_6}$  in Fig. 11. As expected, it drops as  $m_{\Delta_6}$  grows in order to suppress corresponding growth of  $|g_6^{13}|$ .

Before we turn to numerical analysis we stress that all our previous observations do not depend on exact values of up-quark masses.

### A. Numerical analysis

To generate our numerical results shown in Figs. 8, 9, 10 and 11 we have turned to a specific scenario comprising **45**  $\equiv (\Delta_1, \Delta_2, \Delta_3, \Delta_4, \Delta_5, \Delta_6, \Delta_7) = (\mathbf{8}, \mathbf{2}, 1/2) \oplus (\bar{\mathbf{6}}, \mathbf{1}, -1/3) \oplus (\mathbf{3}, \mathbf{3}, -1/3) \oplus (\bar{\mathbf{3}}, \mathbf{2}, -7/6) \oplus (\mathbf{3}, \mathbf{1}, -1/3) \oplus (\bar{\mathbf{3}}, \mathbf{1}, 4/3) \oplus (\mathbf{1}, \mathbf{2}, 1/2)$ , **5**  $\equiv (\Psi_D, \Psi_T) = (\mathbf{1}, \mathbf{2}, 1/2) \oplus (\mathbf{3}, \mathbf{1}, -1/3)$  and **24**  $\equiv (\Sigma_8, \Sigma_3, \Sigma_{(3,2)}, \Sigma_{(\bar{3},2)}, \Sigma_{24}) = (\mathbf{8}, \mathbf{1}, 0) \oplus (\mathbf{1}, \mathbf{3}, 0) \oplus (\mathbf{3}, \mathbf{2}, -5/6) \oplus (\bar{\mathbf{3}}, \mathbf{2}, 5/6) \oplus (\mathbf{1}, \mathbf{1}, 0)$  of Higgs and one fermionic adjoint representation [12] **24<sub>F</sub>**  $\equiv (\rho_8, \rho_3, \rho_{(3,2)}, \rho_{(\bar{3},2)}, \rho_{24}) = (\mathbf{8}, \mathbf{1}, 0) \oplus (\mathbf{1}, \mathbf{3}, 0) \oplus (\mathbf{3}, \mathbf{2}, -5/6) \oplus (\bar{\mathbf{3}}, \mathbf{2}, 5/6) \oplus (\mathbf{1}, \mathbf{1}, 0)$ . Recall,  $\Delta_6$  can be light in this model without supersymmetry that employs 24-dimensional fermionic representation [12] to generate neutrino masses via combination of type I [42–46] and type III [47, 48] seesaw mechanisms. (This is a renormalizable version of the model first proposed in [49] and further analyzed in [50, 51].) In fact, we have demonstrated [10] that this scenario predicts proton decay signatures that are very close to the present experimental limits due to partial proton decay lifetime measurements when both  $\Delta_1$  and  $\Delta_6$  are in the range accessible in collider experiments.

Numerical procedure we use to generate particle spectrum aims at an exact 1-loop level gauge coupling unification scenario with maximal possible unification scale  $M_{GUT}$ . It allows for multiple particle thresholds as long as all relevant constraints are satisfied. In particular, we require that  $10^2 \text{ GeV} \leq m_{\Sigma_3}, m_{\Sigma_8}, m_{\Delta_1}, m_{\Delta_2}, m_{\Delta_4}, m_{\Delta_7}, m_{\rho_3}, m_{\rho_{(3,2)}}, m_{\rho_{(\bar{3},2)}} \leq M_{GUT}$ ,  $10^{12} \text{ GeV} \leq m_{\Psi_T}, m_{\Delta_3}, m_{\Delta_5} \leq M_{GUT}$  and  $10^6 \text{ GeV} \leq m_{\rho_8} \leq M_{GUT}$ . Note, the masses of  $\Psi_T$ ,  $\Delta_3$  and  $\Delta_5$  are bounded from below due to the fact that these fields mediate proton decay through the  $d = 6$  operators.  $\rho_8$ , on the other hand, should be heavier than  $10^6 \text{ GeV}$  to accommodate the Big Bang Nucleosynthesis constraints [49]. Finally, the allowed couplings of the fermionic adjoint lead to the following mass relations [12]

$$m_{\rho_8} = \hat{m} m_{\rho_3}, \quad m_{\rho_{(3,2)}} = m_{\rho_{(\bar{3},2)}} = \frac{(1 + \hat{m})}{2} m_{\rho_3}, \quad (29)$$

where  $\hat{m}$  represents a free parameter that describes the mass splitting between  $\rho_8$  and  $\rho_3$  states.

We take the relevant parameter for the adjoint fermion mass spectrum to be  $\hat{m} = 10^{14}$  and set  $m_{\Delta_6} = 400 \text{ GeV}$  and  $m_{\Delta_1} = 1 \text{ TeV}$  to generate particle spectrum of the theory. This set of assumptions together with  $\alpha_3 = 0.1176$ ,  $\alpha^{-1} = 127.906$  and  $\sin^2 \theta_W = 0.23122$  [32] yields  $M_{GUT} = 1.1 \times 10^{16} \text{ GeV}$  and  $\alpha_{GUT}^{-1} = 26.9$ , where  $\alpha_{GUT}$  represents unified gauge coupling at  $M_{GUT}$ . The corresponding particle spectrum reads  $m_{\Delta_2} = 2.6 \text{ TeV}$ ,  $m_{\Delta_3} = 10^{12} \text{ GeV}$ ,  $m_{\Delta_4} = m_{\Delta_5} = 1.1 \times 10^{16} \text{ GeV}$ ,  $m_{\Delta_7} = 10^2 \text{ GeV}$ ,  $m_{\Sigma_3} = 10^2 \text{ GeV}$ ,  $m_{\Sigma_8} = 10^2 \text{ GeV}$ ,  $m_{\Psi_T} = 1.1 \times 10^{16} \text{ GeV}$ ,  $m_{\rho_8} = 5.6 \times 10^{15} \text{ GeV}$ ,  $m_{\rho_3} = 113 \text{ GeV}$  and  $m_{\rho_{(3,2)}} = m_{\rho_{(\bar{3},2)}} = 1.1 \times 10^{16} \text{ GeV}$ . Using that spectrum we find the following values of the up-quark masses and CKM parameters at the GUT scale at 1-loop level:  $m_u = 0.00046 \text{ GeV}$ ,  $m_c = 0.182 \text{ GeV}$ ,

$m_t = 55.4 \text{ GeV}$ ,  $s_{12}^{CKM} = 0.225$ ,  $s_{23}^{CKM} = 0.00394$ ,  $s_{13}^{CKM} = 0.0462$  and  $\delta^{CKM} = 1.185$ . The input values at the  $M_Z$  are  $m_u = 0.0016 \text{ GeV}$ ,  $m_c = 0.628 \text{ GeV}$ ,  $m_t = 171.5 \text{ GeV}$ ,  $s_{12}^{CKM} = 0.2272$ ,  $s_{23}^{CKM} = 0.0422$ ,  $s_{13}^{CKM} = 0.00399$  and  $\delta^{CKM} = 0.995$ . All relevant input parameters, i.e., quark and lepton masses and mixing parameters, and running procedures are specified in Ref. [10].

In this particular regime proton decay contributions are dominated by the color triplets that reside in both **45** and **5**. (See Fig. [1] in Ref. [10].) However, to be able to accurately predict partial decay lifetimes we need to know the coupling strengths of the triplets to the matter. Here, again, we demonstrate that one part—the one related to the up-quark sector—is already well known due to low-energy constraints. We have done the running of all relevant parameters from low scale to high scale only for the  $m_{\Delta_6} = 400 \text{ GeV}$  case and used those values to infer that the overall Yukawa coupling drop from low-scale to the GUT scale is well described by a common factor of 3.5. It is this factor that was used for analysis for different values of  $m_{\Delta_6}$ . We find this approximation well-justified since our main goal is to present generic features of the up-quark Yukawa sector at the GUT scale.

We randomly vary angles and phases of  $U$  to see if relevant constraints on the elements of  $A'$  are satisfied as given in Eqns. (4), (15) and in Fig. 6 adjusted by a factor of 3.5. Once this is done we read off phenomenologically allowed elements of  $S'$ . Our procedure guaranties viable values of the up-quark masses and CKM mixing parameters while  $A'$  components satisfy all low energy constraints. Note, since we know  $V_{CKM}$  at the GUT scale, we can also reproduce  $U_R$  (up to some phases of diagonal unitary matrices).

All in all, we have generated  $10^8$  random points in the nine-dimensional space of the unitary matrix  $U$  for different values of  $\Delta_6$  mass, i.e.,  $m_{\Delta_6} = 200, 400, 700, 1000 \text{ GeV}$ . For example, when  $m_{\Delta_6} = 400 \text{ GeV}$  we find that out of  $10^8$  sets of initial values of parameters of  $U$ , i.e., the angles and phases of unitary matrix, only 657 pass all phenomenological constraints which implies rather unique form of Yukawa couplings. Due to the fact that our antisymmetric matrix  $A'$  is highly skewed with  $|A'_{13}|$  element being dominant and the fact that the symmetric element  $|S'_{13}|$  is much larger than both  $|S'_{12}|$  and  $|S'_{23}|$  elements we have a situation that the underlying matrix  $M_U$  as given in Eq. (27) in the down-quark mass eigenstate basis is of the so-called lopsided form. (Recall,  $|S'_{13}|$  or equivalently  $|A'_{13}|$  is either comparable or larger than  $|S_{33}|$ .)

Our results for the underlying Yukawa structure of the up-quark sector exhibit dependence on  $v_{45}$  (or  $|U_{31}| = 4|g_6^{13}|v_{45}/m_t$ ). This, as we discuss, provides basis for analytic correlation between all entries of  $S'$  and  $A'$ , except for  $|S'_{23}|$ . In order to appreciate the advantage of this analytic study, we bracket the range of values that these entries can take by resorting to our numerical analysis. We present these ranges, without correlation, for  $m_{\Delta_6} = 400 \text{ GeV}$  and  $m_{\Delta_6} = 1 \text{ TeV}$  in Table I for the absolute values of components of antisymmetric and symmetric contributions. Note that the ranges are more or less  $m_{\Delta_6}$  independent since  $g_6^{ij}$  elements scale similarly with respect to change in  $m_{\Delta_6}$  in the region of interest.

Table I. Allowed ranges of absolute values of relevant components of  $A'$  and  $S'$  in  $m_t$  units for  $m_{\Delta_6} = 400 \text{ GeV}$  and  $m_{\Delta_6} = 1 \text{ TeV}$ .

	$m_{\Delta_6} = 400 \text{ GeV}$	$m_{\Delta_6} = 1 \text{ TeV}$
$ A'_{12} /m_t$	$[2.9 \times 10^{-7}, 8.0 \times 10^{-4}]$	$[1.1 \times 10^{-6}, 8.2 \times 10^{-4}]$
$ A'_{13} /m_t$	$[3.7 \times 10^{-2}, 2.5 \times 10^{-1}]$	$[1.8 \times 10^{-2}, 2.5 \times 10^{-1}]$
$ A'_{23} /m_t$	$[1.4 \times 10^{-5}, 5.6 \times 10^{-4}]$	$[1.4 \times 10^{-5}, 5.1 \times 10^{-4}]$
$ S'_{11} /m_t$	$[2.2 \times 10^{-9}, 4.0 \times 10^{-6}]$	$[5.3 \times 10^{-9}, 3.9 \times 10^{-6}]$
$ S'_{12} /m_t$	$[2.6 \times 10^{-7}, 8.1 \times 10^{-4}]$	$[6.5 \times 10^{-7}, 8.2 \times 10^{-4}]$
$ S'_{13} /m_t$	$[3.7 \times 10^{-2}, 2.5 \times 10^{-1}]$	$[1.8 \times 10^{-2}, 2.5 \times 10^{-1}]$
$ S'_{22} /m_t$	$[5.9 \times 10^{-5}, 1.7 \times 10^{-3}]$	$[1.0 \times 10^{-4}, 1.6 \times 10^{-3}]$
$ S'_{23} /m_t$	$[1.7 \times 10^{-5}, 2.2 \times 10^{-3}]$	$[3.2 \times 10^{-5}, 2.1 \times 10^{-3}]$
$ S'_{33} /m_t$	$[1.2 \times 10^{-3}, 4.9 \times 10^{-1}]$	$[3.3 \times 10^{-3}, 5.0 \times 10^{-1}]$

To summarize, we have shown that the phenomenological constraints on the form of  $A'$  put limitations on allowed form of  $S'$ , i.e., the symmetric contribution to the up-quark masses. In fact,  $|S'_{12}|$ ,  $|S'_{13}|$ ,  $|S'_{33}|$  and  $|S'_{11}|/|S'_{22}|$  are tied to the value of one parameter only, i.e.  $|U_{31}|$  (or, equivalently,  $v_{45}$ ). We have shown corresponding ranges of values of  $|A'|$  and  $|S'|$  elements in Table I for all possible  $v_{45}$ . Clearly,  $v_{45}$  cannot be determined although its upper bound drops as a function of  $m_{\Delta_6}$ . This bound will merge with the lower bound on  $v_{45}$  for a rather large value of  $m_{\Delta_6}$ , when  $\Delta_6$  is out of reach of accelerator experiments and  $|g_6^{13}|$  becomes too large to be trusted. However, additional constraints on the form of Yukawa couplings in the charged lepton and down-quark sector would further reduce the available parameter space for  $v_{45}$ . If and when  $v_{45}$  is better known, we would be able to bracket  $S'$  elements within a narrower range of values.

Note that  $\Delta_6$ , being a part of 45-dimensional representation of  $SU(5)$ , is also a part of a 120-dimensional representation of  $SO(10)$  [52, 53] that is frequently used to generate antisymmetric Yukawa contributions to charged fermion

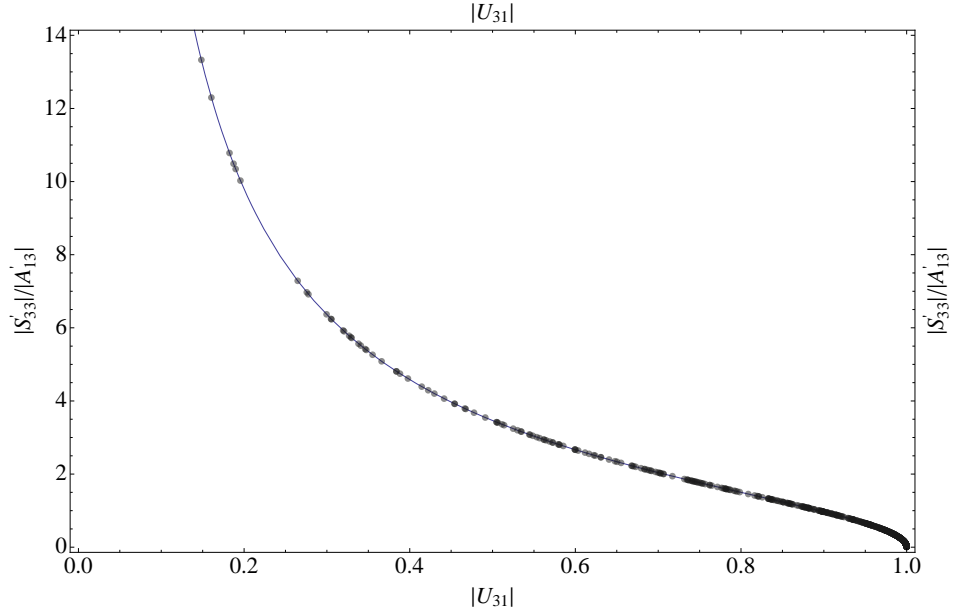


Figure 8. Plot of  $|U_{31}|$  vs.  $|S'_{33}|/|A'_{13}|$ . Squares represent results of our numerical analysis as described in the text whereas the curve stands for approximate analytic expression  $2\sqrt{1-|U_{31}|^2}/|U_{31}|$ . The observed agreement implies that  $|U_{32}|$  is negligible.

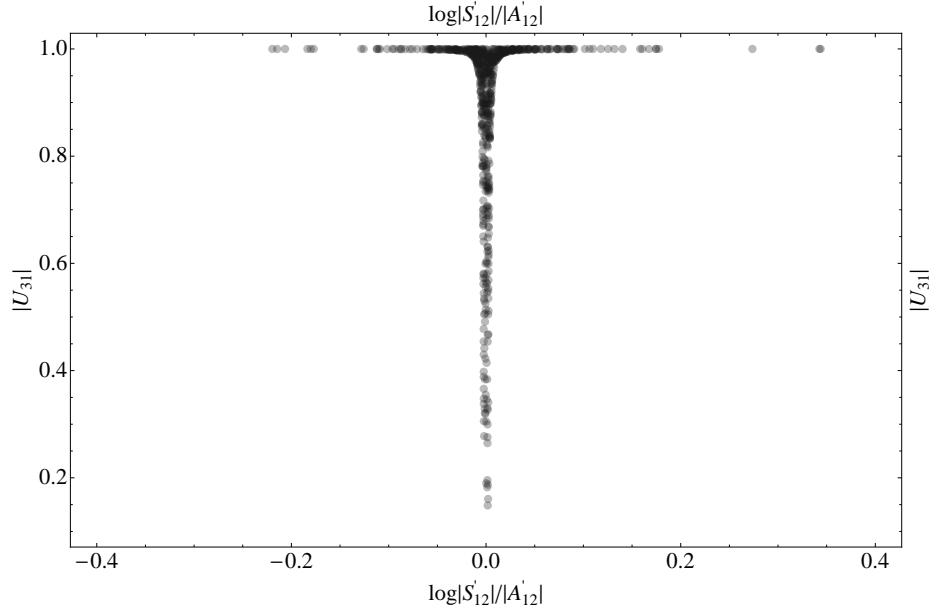


Figure 9. Plot of  $\log |S'_{12}|/|A'_{12}|$  vs.  $|U_{31}|$ . There exist a lower bound on  $|U_{31}|$  due to the fact that  $|A'_{13}| > |A'_{23}|$ . See text for details.

masses. There, in the  $SO(10)$  framework, the symmetry dictates that the antisymmetric contributions to charged leptons, down-quarks and up-quarks are all proportional to the one and the same underlying Yukawa coupling matrix that, on the other hand, is proportional to  $g_6$ . In such a setup one might have additional constraints that could prove sufficient enough to pinpoint the exact Yukawa structure. In fact, the lopsided structures within the  $SO(10)$  framework are known to connect small angles in the quark sector with large angles in the leptonic sector [54] in a natural way. We leave this issue for the future publication.

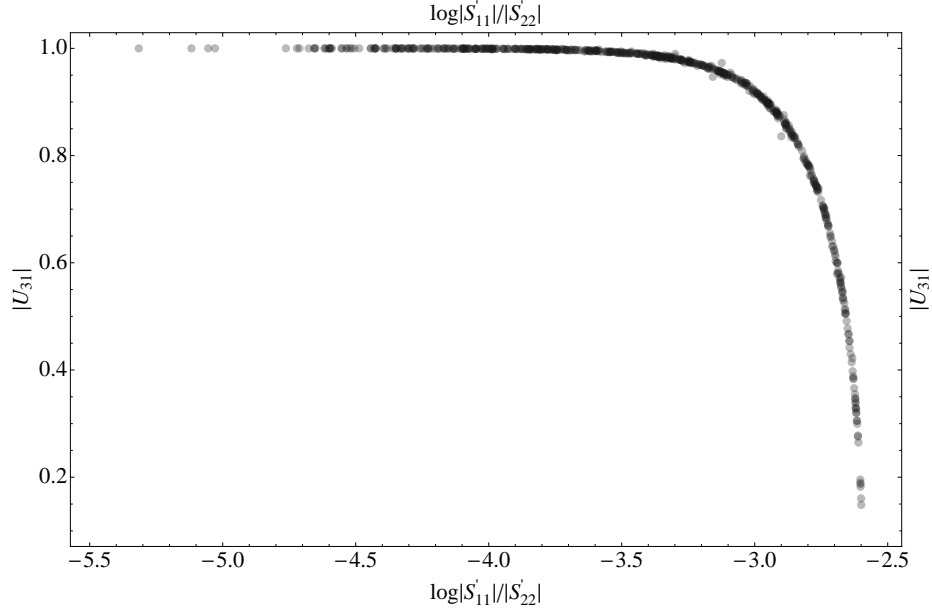


Figure 10. Plot of  $\log |S'_{11}|/|S'_{22}|$  vs.  $|U_{31}|$ .  $|S'_{11}|/|S'_{22}| \rightarrow m_u/m_c$  for small  $|U_{31}|$ .

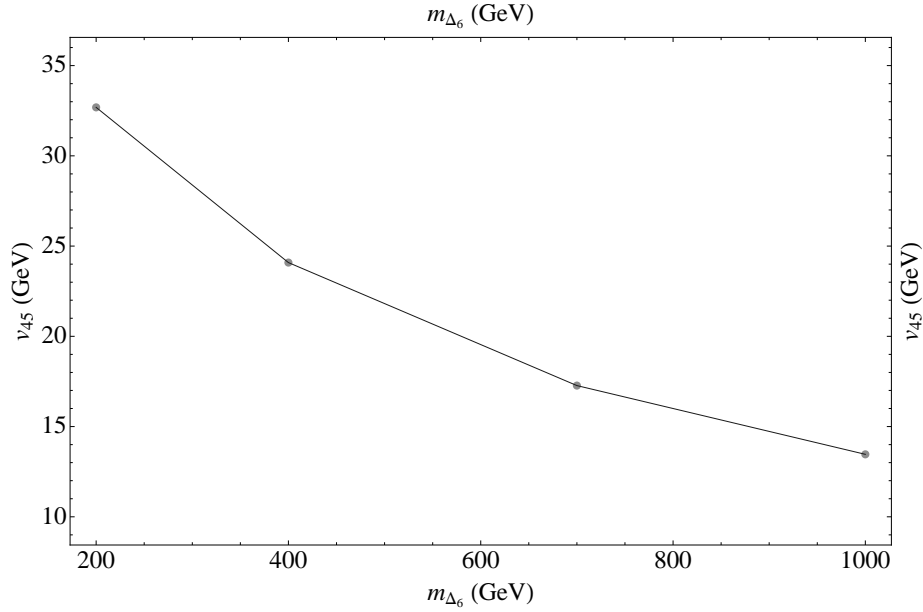


Figure 11. The dependence of upper bound on  $v_{45}$  as a function of  $m_{\Delta_6}$ . Note that  $v_{45}$  drops as  $m_{\Delta_6}$  grows to decrease the influence of the antisymmetric components of  $g_6$  towards the up-quark mass relations.

## VII. SUMMARY

We have investigated flavor constraints and predictions in the presence of the light colored weak singlet scalar, i.e.,  $\Delta_6 = (\bar{3}, 1, 4/3)$ , that couples antisymmetrically, via Yukawa coupling matrix  $g_6$ , to the up-quark sector. A tree-level exchange of  $\Delta_6$  contributes to  $t\bar{t}$  production cross-section in the  $u$ -channel and, when below 1 TeV, can thus enhance the SM prediction of the forward-backward asymmetry  $A_{FB}^{t\bar{t}}$  while not altering the production cross-section  $\sigma_{t\bar{t}}$ . This relates the strength of  $g_6^{13}$  to the  $\Delta_6$  mass via  $|g_6^{13}| = 0.9 + 2.5(m_{\Delta_6}/1 \text{ TeV})$ .

Flavor processes that are sensitive to  $\Delta_6$  exchange offer a way to place bounds on the remaining two couplings in  $g_6$ . Namely, the box diagram consisting of  $\Delta_6$  and  $t$ -quark exchanges mediates  $D^0-\bar{D}^0$  transitions that allow for bound extraction of  $g_6^{23}$ . The bound is phase dependent as summarized in Fig. 3 but,  $|g_6^{23}|$  cannot exceed  $3.8 \times 10^{-3}$

for  $m_{\Delta_6} = 1$  TeV. The CDF search for resonances in the invariant mass spectrum of di-jets as well as the single top production cross-section measurements at the Tevatron put bounds on the coupling  $g_6^{12}$ . We show the relevant bounds on  $|g_6^{12}|$  in Fig. 6.

Having obtained the upper bounds on  $g_6^{12}$  and  $g_6^{23}$  we have also assessed the prospects of looking for radiative top quark decays at the LHC. For  $\Delta_6$  masses below 1 TeV scale we have found the maximal branching fractions of  $t \rightarrow c\gamma$  and  $t \rightarrow cG$  of the order of  $10^{-9}$ , whereas  $t \rightarrow u\gamma$  and  $t \rightarrow uG$  branching fractions are suppressed by an additional 6 orders of magnitude, owing to strong constraints coming from  $D^0-\bar{D}^0$  mixing.

These bounds offer an opportunity to constrain the up-quark Yukawa sector if the weak singlet color scalar has a GUT origin. We have addressed these constraints within a general  $SU(5)$  framework that employs one 5- and one 45-dimensional Higgs representation. Since  $g_6$  is tied to the antisymmetric contribution of the Higgs doublet in the 45-dimensional representation we have deduced the form of the symmetric Yukawa couplings of the 5-dimensional Higgs representation to the matter. We have first described generic features of and correlations between the symmetric Yukawa couplings that are then confirmed numerically by using a particular—theoretically well-motivated—GUT model. We have finally specified the allowed ranges of both symmetric and antisymmetric Yukawa couplings in units of  $m_t$  within that framework. Our setup is unique since the low-energy phenomenological constraints allow us to specify Yukawa couplings in the up-quark sector with great accuracy at the scale of unification.

### ACKNOWLEDGMENTS

This work is supported in part by the European Commission RTN network, Contract No. MRTN-CT-2006-035482 (FLAVIANet) and partially by the Slovenian Research Agency. I.D. would like to thank Jožef Stefan Institute for hospitality where part of this work was completed.

- 
- [1] E. Golowich, J. A. Hewett, S. Pakvasa, and A. A. Petrov, Phys. Rev. **D79**, 114030 (2009), 0903.2830.
  - [2] A. F. Falk, Y. Grossman, Z. Ligeti, Y. Nir, and A. A. Petrov, Phys. Rev. **D69**, 114021 (2004), hep-ph/0402204.
  - [3] O. Gedalia, Y. Grossman, Y. Nir, and G. Perez, Phys. Rev. **D80**, 055024 (2009), 0906.1879.
  - [4] I. I. Bigi, M. Blanke, A. J. Buras, and S. Recksiegel, JHEP **07**, 097 (2009), 0904.1545.
  - [5] Y. Grossman, A. L. Kagan, and Y. Nir, Phys. Rev. **D75**, 036008 (2007), hep-ph/0609178.
  - [6] I. I. Bigi (2009), 0907.2950.
  - [7] A. A. Petrov (2010), 1003.0906.
  - [8] W. Bernreuther, J. Phys. **G35**, 083001 (2008), 0805.1333.
  - [9] J. A. Aguilar-Saavedra, Nucl. Phys. **B837**, 122 (2010), 1003.3173.
  - [10] I. Dorsner, S. Fajfer, J. F. Kamenik, and N. Kosnik, Phys. Rev. **D81**, 055009 (2010), 0912.0972.
  - [11] H. Georgi and S. L. Glashow, Phys. Rev. Lett. **32**, 438 (1974).
  - [12] P. Fileviez Perez, Phys. Lett. **B654**, 189 (2007), hep-ph/0702287.
  - [13] J. M. Arnold, M. Pospelov, M. Trott, and M. B. Wise, JHEP **01**, 073 (2010), 0911.2225.
  - [14] J. Shu, T. M. P. Tait, and K. Wang, Phys. Rev. **D81**, 034012 (2010), 0911.3237.
  - [15] H. Georgi and C. Jarlskog, Phys. Lett. **B86**, 297 (1979).
  - [16] I. Dorsner, S. Fajfer, J. F. Kamenik, and N. Kosnik, Phys. Lett. **B682**, 67 (2009), 0906.5585.
  - [17] K. S. Babu and E. Ma, Phys. Lett. **B144**, 381 (1984).
  - [18] A. Giveon, L. J. Hall, and U. Sarid, Phys. Lett. **B271**, 138 (1991).
  - [19] I. Dorsner and P. Fileviez Perez, Phys. Lett. **B642**, 248 (2006), hep-ph/0606062.
  - [20] I. Dorsner and I. Mocioiu, Nucl. Phys. **B796**, 123 (2008), 0708.3332.
  - [21] M. Ciuchini et al., Nucl. Phys. **B523**, 501 (1998), hep-ph/9711402.
  - [22] R. Gupta, T. Bhattacharya, and S. R. Sharpe, Phys. Rev. **D55**, 4036 (1997), hep-lat/9611023.
  - [23] B. I. Eisenstein et al. (CLEO), Phys. Rev. **D78**, 052003 (2008), 0806.2112.
  - [24] E. Barberio et al. (Heavy Flavor Averaging Group) (2008), 0808.1297.
  - [25] Y. Grossman, Y. Nir, and G. Perez, Phys. Rev. Lett. **103**, 071602 (2009), 0904.0305.
  - [26] S. Fajfer, N. Kosnik, and S. Prelovsek, Phys. Rev. **D76**, 074010 (2007), 0706.1133.
  - [27] G. Burdman, E. Golowich, J. Hewett, and S. Pakvasa, Phys. Rev. **D52**, 6383 (1995), hep-ph/9502329.
  - [28] G. Burdman, E. Golowich, J. Hewett, and S. Pakvasa, Phys. Rev. **D66**, 014009 (2002), hep-ph/0112235.
  - [29] T. Aaltonen et al. (CDF), Phys. Rev. **D79**, 112002 (2009), 0812.4036.
  - [30] T. E. W. Group (CDF) (2009), 0908.2171.
  - [31] H. L. Lai et al. (CTEQ), Eur. Phys. J. **C12**, 375 (2000), hep-ph/9903282.
  - [32] C. Amsler et al. (Particle Data Group), Phys. Lett. **B667**, 1 (2008).
  - [33] T. Kluge, K. Rabbertz, and M. Wobisch (2007), in Proceedings of the 14th International Workshop on Deep Inelastic Scattering (DIS 2006), Tsukuba, Japan, 2006, hep-ph/0609285.

- [34] D. Stump et al., JHEP **10**, 046 (2003), hep-ph/0303013.
- [35] T. Aaltonen et al. (CDF), Phys. Rev. Lett. **101**, 202001 (2008), 0806.2472.
- [36] V. M. Abazov et al. (D0), Phys. Rev. Lett. **100**, 142002 (2008), 0712.0851.
- [37] CDF, public note 9724 (2009).
- [38] V. M. Abazov et al. (D0) (2010), 1006.3575.
- [39] J. J. Zhang et al., Phys. Rev. Lett. **102**, 072001 (2009), 0810.3889.
- [40] J. Drobnak, S. Fajfer, and J. F. Kamenik, Phys. Rev. Lett. **104**, 252001 (2010), 1004.0620.
- [41] J. J. Zhang et al. (2010), 1004.0898.
- [42] P. Minkowski, Phys. Lett. **B67**, 421 (1977).
- [43] T. Yanagida (1979), in Proceedings of the Workshop on the Baryon Number of the Universe and Unified Theories, Tsukuba, Japan, 13-14 Feb 1979.
- [44] M. Gell-Mann, P. Ramond, and R. Slansky (1980), print-80-0576 (CERN).
- [45] S. L. Glashow, NATO Adv. Study Inst. Ser. B Phys. **59**, 687 (1980).
- [46] R. N. Mohapatra and G. Senjanovic, Phys. Rev. Lett. **44**, 912 (1980).
- [47] R. Foot, H. Lew, X. G. He, and G. C. Joshi, Z. Phys. **C44**, 441 (1989).
- [48] E. Ma, Phys. Rev. Lett. **81**, 1171 (1998), hep-ph/9805219.
- [49] B. Bajc and G. Senjanovic, JHEP **08**, 014 (2007), hep-ph/0612029.
- [50] I. Dorsner and P. Fileviez Perez, JHEP **06**, 029 (2007), hep-ph/0612216.
- [51] B. Bajc, M. Nemevsek, and G. Senjanovic, Phys. Rev. **D76**, 055011 (2007), hep-ph/0703080.
- [52] R. N. Mohapatra and B. Sakita, Phys. Rev. **D21**, 1062 (1980).
- [53] R. Slansky, Phys. Rept. **79**, 1 (1981).
- [54] K. S. Babu and S. M. Barr, Phys. Lett. **B381**, 202 (1996), hep-ph/9511446.